

Stress-Induced Positive Charge in Hf-Based Gate Dielectrics: Impact on Device Performance and a Framework for the Defect

Ce Z. Zhao, Jian F. Zhang, Mo Huai Chang, A. R. Peaker, Stephen Hall, *Member, IEEE*, Guido Groeseneken, *Fellow, IEEE*, Luigi Pantisano, Stefan De Gendt, and Marc Heyns

Abstract—A Hf-based dielectric has been selected to replace SiON for CMOS technologies. When compared with SiON, Hf dielectrics can suffer from higher instability. Previous attentions were focused on electron trapping, and positive charging received less attention. The objective of this paper is to study the impact of positive charging on device performance and to provide a framework for the defect. Three components of threshold voltage instability ΔV_{th} are unambiguously identified for pMOSFETs, i.e., loop, loop-shift, and up-loop. The loop dominates ΔV_{th} at a relatively short time (< 1 s). After stressing for a longer time, the whole loop is shifted in the negative direction. Unlike the loop, the up-loop cannot readily be recharged after recovery. In addition to the generated interface states, three different types of positive charges are formed in the Hf-based stacks, i.e., cyclic positive charges (CPC), antineutralization positive charges (ANPC), and as-grown hole trapping (AHT). Each type of defect has its unique signatures and properties. CPC can repeatedly be charged and discharged by alternating the gate bias polarity. ANPC is more difficult to neutralize, whereas AHT is harder to charge. Both the generated interface states and the AHT saturate at longer stress time, but ANPC does not. ANPC reduces at higher measurement temperature, but CPC is insensitive to temperature. The relation between each type of defect and each component of ΔV_{th} is clarified.

Index Terms—Degradation, gate stacks, HfO₂, hf-silicates, negative bias temperature instability (NBTI), positive charges, traps.

I. INTRODUCTION

AS THE thickness of silicon oxynitrides approaches 1 nm, the gate leakage current becomes intolerable. To keep the

Manuscript received October 9, 2007; revised April 16, 2008. This work was supported by the Engineering and Physical Science Research Council of U.K. under Grant EP/C003071/1, Grant EP/C003098/1, and Grant EP/C003101/1, which form a joint research project linking Liverpool John Moores, Liverpool, and Manchester Universities. The review of this paper was arranged by Editor J. Suehle.

C. Z. Zhao was with The School of Engineering, Liverpool John Moores University, L3 3AF Liverpool, U.K. He is now with the University of Liverpool, L69 3BX Liverpool, U.K.

J. F. Zhang and M. H. Chang are with the School of Engineering, Liverpool John Moores University, L3 3AF Liverpool, U.K. (e-mail: J.F.Zhang@ljmu.ac.uk).

A. R. Peaker is with the Centre for Electronic Materials, University of Manchester, M60 1QD Manchester, U.K.

S. Hall is with the Department of Electrical Engineering and Electronics, University of Liverpool, L69 3GJ Liverpool, U.K.

G. Groeseneken, S. De Gendt, and M. Heyns are with the Interuniversity Microelectronics Center (IMEC), 3001 Leuven, Belgium, and also with Katholieke Universiteit, 3001 Leuven, Belgium.

L. Pantisano is with IMEC, 3001 Leuven, Belgium.
Digital Object Identifier 10.1109/TED.2008.925151

downscaling of MOSFETs on track of Moore's law, there is a pressing need for replacing SiON by a gate dielectric of higher dielectric constant (high- k). This has motivated a worldwide research in high- k layers since 1990s [1]–[5]. After investigating many different materials, the Hf-based dielectrics have been selected as the gate dielectric for CMOS technologies. When compared with SiON, Hf dielectrics suffer from lower carrier mobility and higher instability [1]–[5].

On the instability, both electron trapping [3]–[6] and positive charging [7]–[11] in Hf-based dielectrics have been reported. The electron trapping is highly dynamic [5], [6], [12] and rapidly reduces as the Hf dielectrics become thinner [4], [13], [14]. When compared with electron trapping, the stress-induced positive charging received relatively less attention. Positive charging is rarely observed for nMOSFETs due to the masking effects of electron trapping [9]–[11], although it contributes to the negative bias temperature instability (NBTI) of pMOSFETs [7]–[10]. For sub-2-nm Hf dielectric, we will show that positive charging can lead to larger V_{th} instability for pMOSFETs than the electron trapping-induced instability of nMOSFETs. Despite its importance, our understanding of the positive charging is poor. Its impact on device performance is not fully understood, and there is little information on the defect. The objective of this paper is to address these issues and to provide a framework for the defect.

We will report clear results, showing that the instability in threshold voltage ΔV_{th} of pMOSFETs has three components. The first one appears as a “loop” in the two transfer characteristics (TCs) measured during the rising and falling edges of a gate voltage pulse, similar to the V_{th} instability observed for nMOSFETs [1], [5], [6], [12]. It dominates the instability at short time (< 1 s). The second is a shift of the whole loop, and the third is an up-loop, which counts for the difference between the total ΔV_{th} and the sum of the loop and loop-shift.

On the defect, historically, positive charging in SiO₂ has puzzled the international community for decades. Some positive charges behave so strangely that they are called by various names, such as anomalous positive charges [15], slow states [16], and border traps [17]. It has recently been reported that the anomalous behavior originates from the simultaneous presence of different types of positive charges in SiO₂, i.e., cyclic positive charge (CPC), antineutralization positive charge (ANPC), and as-grown hole trapping (AHT) [18]–[20]. For Hf-based dielectrics, there are two questions. One is whether the same types

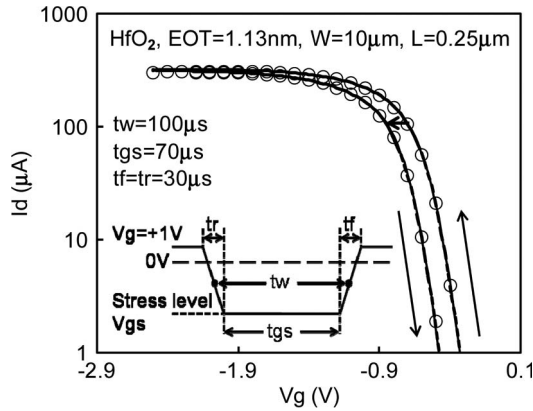


Fig. 1. TCs corresponding to the two edges of a gate bias pulse shown in the inset. The rising and falling time is $30 \mu\text{s}$, and the peak time is $70 \mu\text{s}$, giving a pulse width of $100 \mu\text{s}$. The negative shift of the falling TC from the rising TC indicates positive charge formation. The solid lines represent the TCs when the gate pulse was applied to a fresh device. The dashed lines represent the TCs when the same pulse was applied again. The symbol “o” represents the TCs obtained by applying quasi-dc V_g ramps, where V_g was ramped from $+1$ to -2.5 V in 4 s and then back to $+1$ V.

of defects also exist. If this is true, the other question is what is the relation between each type of defect and the three components of ΔV_{th} . These questions will be answered in this paper.

II. DEVICES AND EXPERIMENTS

A. Devices

For a 3-nm or thicker Hf layer, electron trapping and positive charging can simultaneously occur [9], [10]. This is highly undesirable for studying positive charges, since electron trapping compensates positive charging and complicates the analysis. To simplify the test condition, electron trapping should be suppressed. Recent work [4], [13] shows that electron trapping is substantially suppressed in 2-nm or thinner Hf layers. As a result, 2-nm or thinner Hf layers are selected as test samples in this paper.

Both HfO_2 and Hf-silicate were prepared by atomic layer deposition. Before depositing HfO_2 , the chemical SiO_2 was nitrided in NH_3 at 900°C for 60 s. A 2-nm HfO_2 was then prepared, resulting in an equivalent oxide thickness (EOT) of 1.13 nm. For the Hf-silicate, a 1-nm HfSiO (70% Hf) layer was deposited and then nitrided in NH_3 at 800°C for 60 s, giving an EOT of 1.3 nm. A 1000°C spike was used to activate the source and drain dopant, and the gate is TaN. The channel length and width of pMOSFETs is $0.25\text{--}1$ and $10 \mu\text{m}$, respectively.

To facilitate the comparison, nMOSFETs were also prepared with 2-nm HfO_2 . The gate metal, channel length, and width are the same as those of pMOSFETs. A 5.5-nm SiO_2 and a 2.7-nm SiON were also used for comparison.

B. Experiments

Both the pulsed $I_d \sim V_g$ [5], [6], [12] and the traditional quasi-dc $I_d \sim V_g$ [21], [22] were used to monitor the positive charge. The waveform of the gate pulse used is given in the inset of Fig. 1. The gate bias was ramped from $+1$ V to a stress level of V_{gs} and stayed at V_{gs} for a time of t_{gs} before

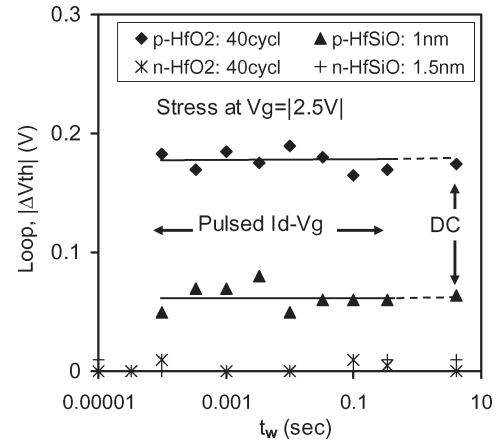


Fig. 2. Dependence of loop size $|\Delta V_{th}|$ on the gate pulse width t_w . The measurement time is proportional to t_w , and the $|\Delta V_{th}|$ is clearly insensitive to t_w . The quasi-dc measurement was obtained by applying two voltage ramps, and the ramp time is 4 s. The instability of pMOSFETs can substantially be higher than that of nMOSFETs for sub-2-nm Hf dielectrics.

being ramped back to $+1$ V in a time of t_f . “ t_w ” is the pulse width. For the quasi-dc $I_d \sim V_g$, the ramp time is 4 s, and the t_{gs} is 0.15 s. As shown in Fig. 1, the shift of the threshold voltage ΔV_{th} is assessed at a fixed drain current of 10^{-5} A with a drain bias of -0.1 V for both pulse and quasi-dc tests. The positive charge in the Hf stack is evaluated from the shift of gate voltage at midband of silicon [23], [24]. Since the distribution of positive charge within the Hf stack is not known, we follow the well-accepted practice and use the “effective charge density” ΔN_{ot} by assuming the charge centroid being at the oxide/substrate interface [23], [24]. The generated interface states were assessed from the change in the subthreshold swing [24], [25]. The stress of the Hf dielectric was carried out under a constant gate bias with all the other terminals grounded. For SiO_2 , the substrate hole injection (SHI) [18]–[20] was also used to stress the device. The range of temperature is 25°C to 200°C . In some tests, the stress and measurement temperature was kept the same, but there were also tests where they were different. When ΔV_{th} was evaluated, the stressed and reference $I_d \sim V_g$ were always measured at the same temperature. Further details of the measurement techniques can be found from earlier works [5], [6], [12], [18], [21], [22].

III. IMPACT ON DEVICE PERFORMANCE

In this section, we will show that the positive charging-induced ΔV_{th} has three components, i.e., loop, loop-shift, and up-loop.

A. Loop

Fig. 1 shows the $I_d \sim V_g$ corresponding to the rising and falling edge of a gate voltage pulse given in the inset. When I_d fell, it did not follow the same curve as when I_d rose. $I_d \sim V_g$ is moved in the negative direction, and a “loop” is formed, indicating positive charge formation. When the same pulse was applied again, the dashed lines in Fig. 1 show that the same loop was obtained.

Fig. 2 plots the loop size ΔV_{th} against the pulse width (t_w), and the measurement time is proportional to t_w . It clearly shows that the ΔV_{th} observed here is insensitive to the measurement time in a range from tens of microseconds to seconds. The data marked by “DC” was obtained by using quasi-dc V_g ramps with a ramp time of 4 s. To further illustrate the insensitivity of ΔV_{th} to measurement time, the quasi-dc $I_d \sim V_g$ is given in Fig. 1 as the symbol “o” and it agrees well with the pulsed $I_d \sim V_g$. This is in contrast with the substantial reduction of $|\Delta V_{th}|$ when measured by quasi-dc $I_d \sim V_g$ for both Hf-based nMOSFETs [5], [6], [12], [13] and the pMOSFETs with a SiON gate dielectric [24], [26], [27]. An explanation will be given when we address the defect responsible for the loop in Section IV-C.

The ΔV_{th} of nMOSFETs and pMOSFETs with the same HfO₂ thickness is compared in Fig. 2. It clearly shows that the V_{th} instability of pMOSFETs can be higher. The insignificant $|\Delta V_{th}|$ for nMOSFETs in a sub-2-nm Hf layer agrees with early works [4], [13]. This confirms that any compensation of electron trapping on positive charging is negligible in this paper.

B. Loop-Shift

When the stress time is shorter than 1 s, Fig. 3(a) shows that the loop dominates ΔV_{th} and does not increase with stress time. This is in contrast with the typical NBTI, where the instability increases [28], [29]. For longer stress, ΔV_{th} does increase, but we will show the loop remaining the same.

The gate bias waveform used is given in Fig. 3(b). Initially, two voltage ramps labeled as “A” and “B” were applied, and the corresponding $I_d \sim V_g$ in Fig. 3(c) shows the expected loop. After stressing the device at $V_{gs} = -2.5$ V for 2×10^4 s, three voltage ramps [“C,” “D,” and “E” in Fig. 3(b)] were applied, and the resultant $I_d \sim V_g$ is labeled as “C,” “D,” and “E” in Fig. 3(c). Several observations can be made. First, when V_g was ramped from the stress level toward positive after the long stress (ramp “C”), $I_d \sim V_g$ was shifted further negatively from “B” to “C,” confirming more positive charging during the stress. Second, when V_g was ramped from +1 V in the negative direction (ramp “D”), the difference between “C” and “D” in Fig. 3(c) shows a loss of positive charges, typically referred to as “recovery” [24], [30]. Third, when V_g was ramped toward positive again (ramp “E”), the curve “E” appears between “C” and “D.” The difference between “E” and “C” will be addressed in the next section, and here, we explore the relation of the four $I_d \sim V_g$: “A,” “B,” “D,” and “E.”

Since the ramps “D” and “E” in Fig. 3(b) are the same as the “A” and “B” used to measure the loop, the negative shift from “D” to “E” shows that the loop still exists after the long stress. Furthermore, the difference between “E” and “D,” “E”-“D,” is the same as “B”-“A,” so the loop size is unchanged before and after stress. This indicates that the defects responsible for the loop are cyclic, and their density is not affected by the charging and discharging during the test. However, the stress negatively shifted the whole loop, and the loop-shift can be evaluated either from the two rising $I_d \sim V_g$ (“D”-“A”) or the two falling $I_d \sim V_g$ (“E”-“B”). If the loop-shift is recoverable, one would expect $|“E”-“B”| > |“D”-“A”|$,

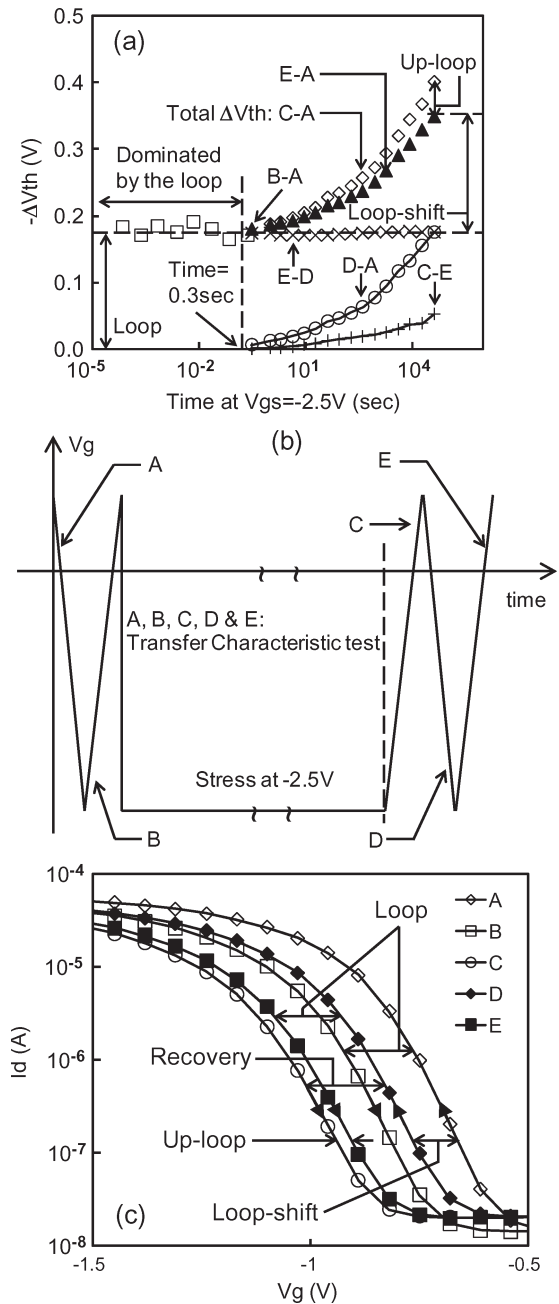


Fig. 3. Separation of three components of V_{th} instabilities: loop, loop-shift, and up-loop. (a) Instability was dominated by the loop at short time, and the loop is insensitive to stress time. The symbol \square was obtained from the pulsed $I_d \sim V_g$ shift. For stress time longer than 0.3 s, the data in (a) were obtained by applying the gate bias given in (b). Here, two V_g ramps labeled “A” and “B” were first applied, and the corresponding $I_d \sim V_g$ is shown as the curve “A” and “B” in (c). After stressing at $V_{gs} = -2.5$ V for a prespecified time, three further V_g ramps labeled as “C,” “D,” and “E” were applied. As an example, the three $I_d \sim V_g$ after a stress time of 2×10^4 s are shown as the curve “C,” “D,” and “E” in (c). The symbol \blacktriangle in (a) is the sum of the loop (\times) and the loop-shift (\circ). The symbol \diamond in (a) is the total V_{th} instability, the sum of the loop (\times), the loop-shift (\circ), and the up-loop ($+$).

since “E” was measured after recharging at $V_g = -2.5$ V. The fact that $|“E”-“B”| = |“D”-“A”|$ indicates that the loop-shift recovery is negligible. Since the loop-shift has no influence on the loop size, the loop and the loop-shift must originate from different types of defect, which will be further investigated in Section IV. Fig. 3(c) was obtained after a stress time of

2×10^4 s. Fig. 3(a) shows the evolution from a fresh device to Fig. 3(c). The loop size clearly remains the same during the stress, but both the loop-shift and the up-loop increase with stress time.

C. Up-Loop

The traditional NBTI is the total ΔV_{th} , namely, “C”–“A” in Fig. 3(c), and it can be divided into

$$\Delta V_{th}('C' - 'A', Total) = \Delta V_{th}('D' - 'A', loop-shift) + \Delta V_{th}('C' - 'D', Recovery).$$

As described earlier, the loop-shift does not recover. The recoverable part consists of two components

$$\Delta V_{th}('C' - 'D', Recovery) = \Delta V_{th}('E' - 'D', Loop) + \Delta V_{th}('C' - 'E', Up-loop).$$

To find out the difference between these two, we reexamine Fig. 1. When the same gate pulse was applied twice, the same rising and falling $I_d \sim V_g$ were obtained. The good agreement for the two rising $I_d \sim V_g$ indicates that the application of $V_g = +1$ V at the end of the first pulse led to a full neutralization of relevant defect, and consequently, the loop is recoverable. The good agreement for the two falling $I_d \sim V_g$ means that the defects responsible for the loop were fully recharged during the second pulse. This is in contrast with Fig. 3(c), where the difference between “C” and “E” indicates that some defects were not recharged by reapplying a V_g ramp after neutralization. This component “C”–“E” will be referred to as “up-loop” hereafter. The stress time is less than 1 s for Fig. 1 and 2×10^4 s for Fig. 3(c). Fig. 3(a) shows that the up-loop (“C”–“E”) is negligible at short time (< 1 s) and builds up as the stress time increases. In Section IV, more results will be presented to support that the loop and up-loop originate from different defects.

IV. FRAMEWORK FOR DEFECTS

A. Types of Positive Charge in SiO₂

To have a benchmark for positive charge in Hf stacks, a brief review of the positive charge in SiO₂ will be given. A typical and summarizing result reported for SiO₂ is reproduced in Fig. 4(a) [18]. Here, positive charges were first formed during SHI with an oxide field of $E_{ox} = -5$ MV/cm. A Fowler–Nordheim electron injection was then used to neutralize them. This is followed by alternatively applying $V_g < 0$ and $V_g > 0$ with $E_{ox} = \pm 5$ MV/cm. Under $V_g < 0$, some of the neutralized positive charge can be recharged without resuming hole injection. When the gate bias polarity is switched, part of the positive charge can repeatedly be neutralized and recharged, so that they are called as CPC. The neutralization of some positive charge under $V_g > 0$ is more difficult than their charging under $V_g < 0$, and they are referred to as ANPC.

Fig. 4(b) and (c) shows that the energy level of ANPC is higher than that of CPC and is above the bottom edge of the Si conduction band. This explains the difficulty in neutralizing ANPC. Under the same $E_{ox} = -5$ MV/cm, the recharging

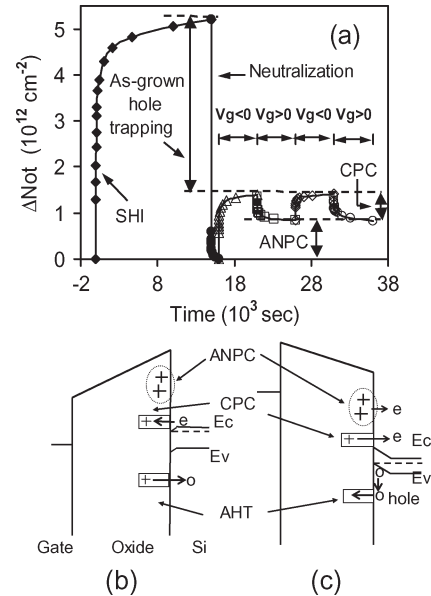


Fig. 4. Presence of three different types of positive charges in a 5.5-nm SiO₂. (a) Test sequence. Initially, positive charging built up during an SHI under an oxide field of $E_{ox} = -5$ MV/cm, an n-well and p-substrate bias of 6 and 7 V, respectively [18]. The neutralization was under $E_{ox} = +8$ MV/cm. This was followed by alternately applying $V_g < 0$ ($E_{ox} = -5$ MV/cm) and $V_g > 0$ ($E_{ox} = +5$ MV/cm), with all the other terminals grounded. The (b) neutralization and (c) charging of CPC only involve electron tunneling at the same energy level. The ANPC has an energy level above the conduction band edge of Si, making its neutralization difficult. For the same $E_{ox} = -5$ MV/cm, the charging level without switching on SHI is well short of that with SHI, since AHT cannot be filled by holes near the top edge of the Si valence band (c).

under $V_g < 0$ without SHI clearly did not reach the level when SHI was switched on. This indicates that some defects are difficult to recharge without accelerating holes in the substrate, as illustrated in Fig. 4(c), and they are AHT [18]–[21].

$E_{ox} = \pm 5$ MV/cm was selected here for the cycled test. An increase of $|E_{ox}|$ will result in a higher CPC. However, the AHT does not depend on this E_{ox} so long as the same E_{ox} is used for sensing during the stress and cycled tests, since the CPC charge is subtracted out when AHT is evaluated, as shown in Fig. 4(a). ANPC does not depend on this E_{ox} either, if the magnitude of $E_{ox} < 0$ and $E_{ox} > 0$ is kept the same. The cyclic nature of CPC means that it is neutralized at the end of $E_{ox} > 0$ period, where ANPC is assessed in Fig. 4(a). More details on how to separate AHT from CPC and ANPC and their different properties can be found in our early works [18]–[21].

B. Types of Positive Charge in Hf-Based Dielectrics

For SiO₂ or SiON, the three types of positive charge were insensitive to either stress or process conditions [18], [24]. For example, Fig. 4(a) was obtained after stressing a 5.5-nm SiO₂ by SHI [18]. The same three types of positive charge were also observed in a 2.7-nm SiON layer after negative bias temperature stress [24]. The question is whether the same types of positive charge can be formed in Hf stacks.

Fig. 5(a) and (b) shows the behavior of positive charges in pMOSFETs with HfO₂ and HfSiON, respectively. The devices were first stressed under $V_g < 0$, and the positive charge built up. Following a neutralization step, the gate bias polarity was

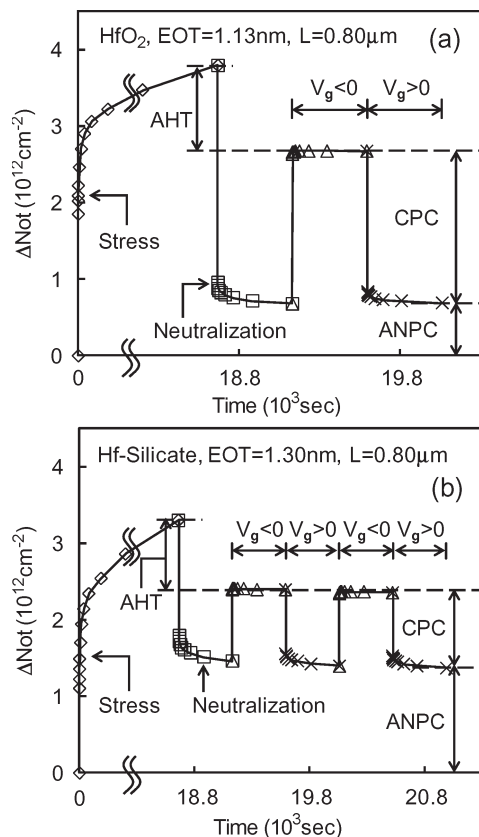


Fig. 5. Types of positive charges in (a) HfO₂ and (b) Hf-silicate (70% Hf). The HfO₂ and Hf-silicate was first stressed for a relatively long time (18 662 s) under $V_g = -2.5$ and -2.8 V, respectively. The stress period is not drawn to scale here. To determine the types of positive charges, the sensing phase started with the neutralization carried out under $E_{ox}(EOT) = +6.5$ MV/cm, followed by applying $V_g < 0$ and $V_g > 0$ corresponding to $E_{ox}(EOT) = \pm 5$ MV/cm, respectively. A comparison with Fig. 4(a) indicates that the same three types of positive charges were formed in SiO₂ and Hf-dielectrics.

alternated, and the magnitude of electrical field across the interfacial layer was kept at 5 MV/cm. The first impression is that the positive charge in both HfO₂ and HfSiON behaves remarkably similar to that in SiO₂, suggesting that the same types of positive charge were formed. Further evidences supporting this statement will be given in the following sections.

A comparison of the curve labeled as “neutralization” for SiO₂ in Fig. 4(a) with that for the Hf-based stacks in Fig. 5(a) and (b) shows that the positive charge was only fully neutralized in the former case. This difference is not fully understood at present. There are two possible reasons, i.e., the inclusion of the high-*k* layer and the reduction in layer thickness. Fig. 4 used a 5.5-nm SiO₂ and Fig. 5(a) used a 2-nm HfO₂ with an EOT of 1.13 nm. If the reduction of thickness is responsible for the difference, one would expect a similar difference if a thinner SiO₂ or SiON is used. Our results [24] confirm that the neutralization was also incomplete for a 2.7-nm SiON film. We speculate that a thinner layer could raise the energy level of ANPC, making its neutralization difficult.

Finally, we would like to point out that, although the Hf stacks used in this paper were nitrated, the same three types of positive charges were observed for Hf stacks without nitridation (not shown). Nitridation does not introduce a new type of positive charges. Although the density of positive charges

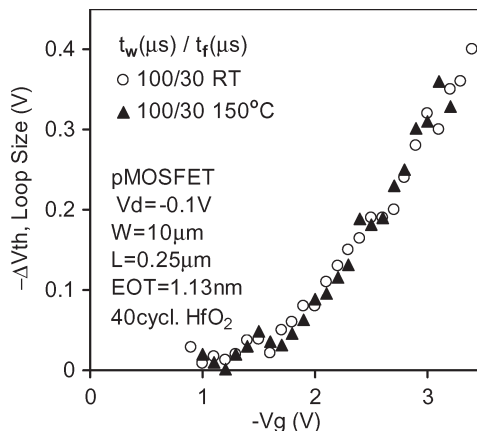


Fig. 6. Dependence of the loop on temperature. In this test, the stress and measurement were at the same temperature. The loop is clearly insensitive to temperature.

depends on process conditions [18], [24], [31], the framework proposed here for positive charges is not process specific. In the following, we will study which type of defect is responsible for each component of ΔV_{th} reported in Section III.

C. Defect for the Loop

As described earlier, the same loop in Fig. 1 was obtained when a gate pulse was applied twice, indicating that the defect can repeatedly be positively charged under $V_g < 0$ and neutralized under $V_g \geq 0$. This suggests that the loop originates from CPC, since all the other types of defects are not cyclic. A key test for this suggestion will be the loop’s dependence on measurement temperature. As illustrated in Fig. 4(b) and (c), the charging and discharging of CPC only involves carrier tunneling at the same energy level. Since tunneling is insensitive to temperature, CPC is insensitive to temperature too, which is confirmed by our early work [18], [24]. If the loop originates from CPC, it must be insensitive to temperature. This is confirmed in Fig. 6. As a result, the loop has all the features of CPC, strongly supporting that it originates from CPC.

To assess the contribution of the generated interface states ΔD_{it} to the loop, we will use both the $I_d \sim V_g$ of pMOSFETs and the high-frequency capacitance–voltage (*CV*) characteristics measured on capacitors with an n-type substrate. $I_d \sim V_g$ and $C \sim V$ allow the assessment of ΔD_{it} in the lower and up half of the silicon bandgap, respectively. Fig. 7 shows $C \sim V$ when V_g was ramped from +1 V to -2.5 V and then back, which is the typical V_g ramp used for measuring the loop. There is little distortion in the $C \sim V$ slope, so that ΔD_{it} is negligible in the up half of the bandgap during loop measurement. A loop cannot be seen in the two $C \sim V$ s since the rise of capacitance occurs when $V_g > 0$. As mentioned earlier, CPC is neutralized under $V_g > 0$ and, consequently, has no effect on $C \sim V$. An inspection of Fig. 1 shows that the rising and falling $I_d \sim V_g$ is in parallel within the subthreshold region. The ΔD_{it} extracted from the subthreshold swing is given in Fig. 8, confirming that ΔD_{it} is also negligible in the lower half of the bandgap when the loop dominates ΔV_{th} .

We now speculate why the loop size ΔV_{th} of the Hf-based pMOSFETs is insensitive to measurement time, unlike

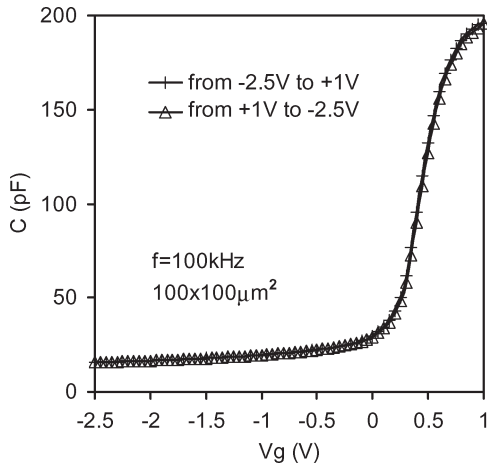


Fig. 7. Capacitance–gate voltage (C – V) characteristics of a MOS capacitor. For a fresh HfO_2 layer, the V_g was ramped from +1 V to –2.5 V and then back, which was typically used to measure the loop for a pMOSFET. The good agreement in the two C – V s indicates that the creation of interface states in the up-half of the silicon bandgap during the measurement is negligible and contributes little to the loop.

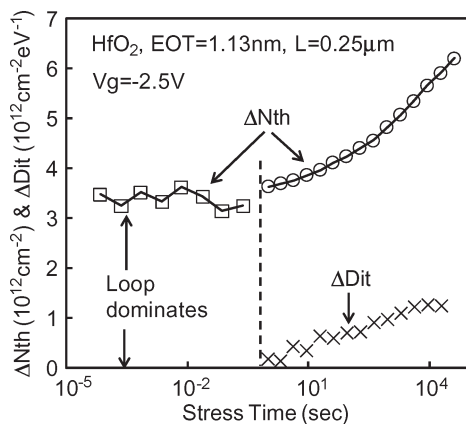


Fig. 8. Contribution of generated interface states ΔDit to the threshold voltage instability ΔV_{th} . $\Delta N_{\text{th}} = |\Delta V_{\text{th}}| \times C_{\text{ox}}/q$, where C_{ox} is the oxide capacitance per unit area, and q is one electron charge. ΔN_{th} is the effective density of total charges by assuming all charges being at the dielectric/substrate interface. ΔDit is negligible when loop dominates but considerable at longer stress time. The test procedure is the same as that in Fig. 3.

Hf-based nMOSFETs and SiON-based pMOSFETs. The dominance of CPC for Hf-based pMOSFETs can throw some light on the difference. Fig. 4(b) shows that the neutralization of CPC requires a supply of free electrons from the substrate. For pMOSFETs, ΔV_{th} is measured under $V_g < 0$, and free electrons are repelled from the dielectric/Si interface. This lack of free electrons at the interface weakens the neutralization of CPC and could be responsible for the insensitivity of CPC to measurement time. For Hf-based nMOSFETs, electrons can be detrapped by tunneling away from the defects, and a supply of carriers is not needed. For SiON-based pMOSFETs, ΔV_{th} at short time is dominated by AHT [24], [26], [32]. Fig. 4(b) shows that the neutralization of AHT requires electrons tunneling from the Si valence band, namely, a hole tunneling away from AHT. Unlike free electrons needed for neutralizing CPC, there are plenty of valence electrons for neutralizing AHT

even under $V_g < 0$ during the measurement, resulting in higher charge losses for longer measurement time.

Finally, it should be pointed out that the insensitivity of the loop to stress time in Figs. 2 and 3 indicates that CPC can preexist in the Hf stacks, whereas early works show that CPC is generated for SiO_2 [18]–[20] and SiON [24]. In this sense, the Hf stacks behave like a stressed SiO_2 .

D. Defect for the Up-Loop

Since CPC is responsible for the loop, we effectively rule out that CPC can contribute to the other two components. This is because the loop and CPC do not increase with stress, but the others do. We now explore which defect is responsible for the up-loop.

Fig. 3(c) shows that both the loop and the up-loop lose their charge when V_g was ramped from the negative stress bias to +1 V. Unlike the loop, the up-loop was not recharged as V_g ramped back to the stress level. This means that the neutralization of the defect is much easier than its charging. An examination of Figs. 4 and 5 indicates that AHT is the only type of defect of such a property and must be responsible for the up-loop. Fig. 4(c) shows that both CPC and ANPC can positively be charged through electron tunneling away from them without involving hot holes, but this does not apply to AHT [18]–[21]. The energy level of AHT is below the top edge of the silicon valence band [33], [34], and AHT cannot be filled by holes at the top edge. Holes must be excited to be able to fill AHT. Since the hole density exponentially reduces away from the top edge, filling AHT is considerably more difficult than charging CPC and ANPC. This explains why the AHT was not recharged by applying a V_g ramp in Fig. 3(c). It also agrees with Fig. 1, where the application of a gate pulse twice does not produce any up-loop, since the pulse width (100 μs) is too short to fill AHT.

To further support that the “AHT” labeled in Fig. 5 is indeed the as-grown hole trap, we next examine its features. Early works [18]–[21] show that AHT should have the following characters: 1) the charging should be negligible at the start of the stress when traps are empty; 2) the charging must saturate as all traps are filled for sufficiently long stress time; and 3) the saturation level should be independent of stress conditions. If the “AHT” in Fig. 5 originates from the as-grown hole trap, it should possess all these characters.

Fig. 5 shows how AHT was assessed. A relatively long stress (18 662 s) was first used to charge the AHT. Both AHT and CPC were then neutralized. This was followed by applying $V_g < 0$ to recharge CPC, but not AHT, allowing their separation. Fig. 9 shows that AHT is negligible at short stress time, and it indeed saturates at longer time, and the saturation level is not sensitive to stress temperature. We found that the saturation was not sensitive to stress bias either (not shown). As a result, AHT has the expected characters of AHT.

The saturation level of AHT in the Hf stack is around $1.4 \times 10^{12} \text{ cm}^{-2}$. This is in the same order as that in a typical SiO_2 [18], and there is no obvious increase of AHT in Hf stacks, in contrast with the orders of magnitude increase of the as-grown electron traps in Hf stacks [5], [35]. The AHT does not appear being correlated with the as-grown electron traps for Hf stacks.

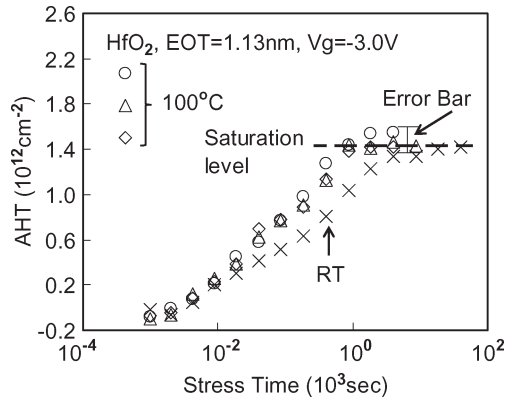


Fig. 9. Dependence of AHT on stress time and temperature. AHT is initially negligible but saturates at a level insensitive to the temperature. The test at 100 °C was repeated on three different devices to give the error bar.

E. Defect for the Loop-Shift

The loop-shift is not neutralized even when V_g is ramped to +1 V. Fig. 5 shows that ANPC has this property. In addition, it is well known that interface states can be created during stress. We will consider the generated interface states first and then ANPC.

- 1) Generated interface states ΔDit : For SiON, it has been suggested that ΔDit can dominate NBTI [36]. To find its contribution to the loop-shift of Hf stacks, Fig. 8 compares ΔDit with the total effective density of positive charges formed under negative bias stress ΔNth . Although ΔDit is negligible at short time (< 1 s), where the loop dominates, it becomes considerable as the stress time increases. However, the instability is not dominated by ΔDit for Hf stacks. ΔDit eventually saturates around $1.3 \times 10^{12} \text{ cm}^{-2} \text{ eV}^{-1}$, broadly agreeing with the well-known inherent density of P_{b0} centers [37] and the stress-induced saturation level for SiO_2/Si interface states [38]. This confirms that the recovery of generated interface states is insignificant in our case. As a result, ΔDit cannot be responsible for the up-loop, which is recoverable.
- 2) ANPC: The ANPC is the positive charge that can survive neutralization even under $V_g > 0$. We will show that it is the only defect responsible for two features of ΔV_{th} , i.e., a reduction for higher measurement temperature and nonsaturation against stress time.

To examine the effect of measurement, rather than stress, temperature on ΔV_{th} , the number of defects should be fixed when varying the measurement temperature. This can be achieved by first annealing a device at the highest measurement temperature (200 °C) for 30 min after stress, during which the initial rapid recovery occurred and the defect density was stabilized [29]. The device was then cooled down to room temperature (25 °C), and the measurement temperature varies in the following sequence:

$$25 \text{ }^\circ\text{C} \rightarrow 65 \text{ }^\circ\text{C} \rightarrow 100 \text{ }^\circ\text{C} \rightarrow 150 \text{ }^\circ\text{C} \rightarrow 200 \text{ }^\circ\text{C}.$$

Fig. 10(a) clearly shows that, for a given number of defects, ΔV_{th} actually progressively reduces as the measurement temperature increases. To confirm that the number of defects

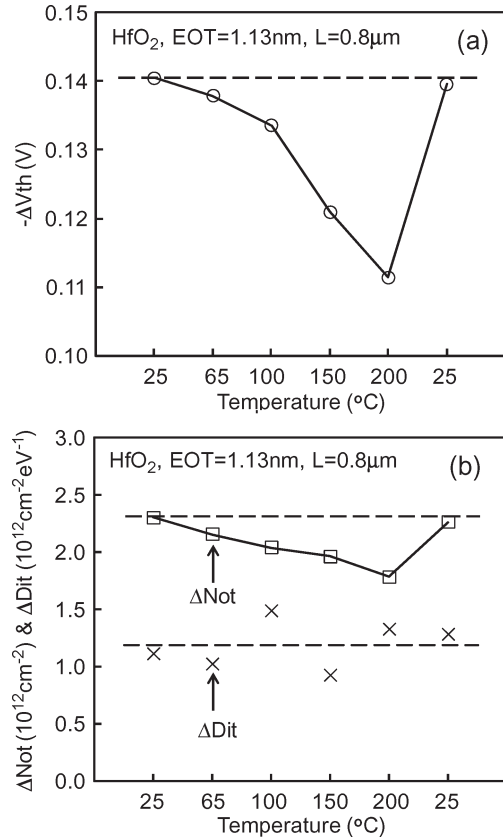


Fig. 10. Dependence of the instability on the measurement temperature. A device was first stressed at $V_g = -2.5$ V for 17 h at 25 °C. It was then annealed at 200 °C for 30 min with gate floating, during which the initial rapid recovery occurred. After stabilization of the defect, the measurement temperature was varied. (a) ΔV_{th} reduces for higher measurement temperature for a given number of defects. (b) The positive charge density ΔNot behaves like ΔV_{th} , but ΔDit is insensitive to measurement temperature.

remain the same during the above temperature sequence, the device was cooled down to 25 °C again after measuring at 200 °C. Fig. 10(a) shows that the ΔV_{th} measured at 25 °C at the start and end of the above sequence agrees well, so the defect density changed little during the above measurement sequence.

To find out the origin of this measurement temperature dependence of ΔV_{th} , Fig. 10(b) shows the dependence of ΔNot and ΔDit on the measurement temperature. ΔDit is insensitive to temperature, whereas ΔNot behaves similar to ΔV_{th} . As a result, the dependence of ΔV_{th} on the measurement temperature originates from the positive charge in Hf stacks.

To show this temperature dependence coming from ANPC, Fig. 11 presents the ANPC measured at different temperatures. It is clear that ANPC is enhanced as the temperature reduces from 150 °C to 25 °C, but CPC remains the same. As shown in Fig. 9, AHT is not responsible for this temperature dependence of ΔV_{th} . Fig. 4(b) illustrates that the energy level of ANPC is above the bottom edge of the silicon conduction band. An increase of temperature enhances the number of electrons that can reach the ANPC and, consequently, reduces the positive charge. This sensitivity to measurement temperature implies that the antineutralization feature of ANPC cannot be explained by assuming it being located further away from the dielectric/substrate interface [9], [10], since tunneling is not sensitive to temperature.

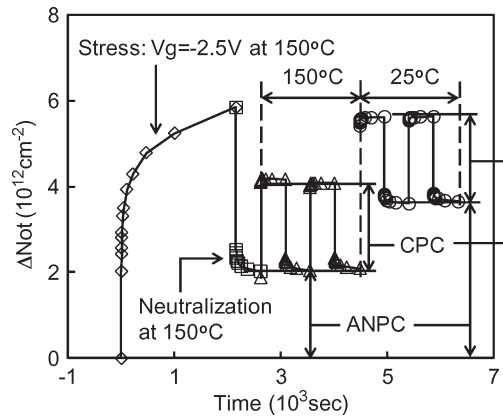


Fig. 11. Dependence of different types of positive charge on measurement temperature. The initial test sequence is the same as that in Fig. 5(a). After measurement at the stress temperature of 150 °C, the device was cooled down to 25 °C, and both CPC and ANPC were assessed again. It is clear that ANPC increases for lower measurement temperature, but CPC does not.

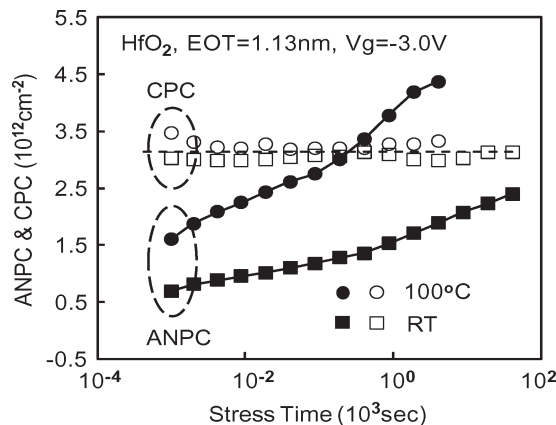


Fig. 12. Dependence of ANPC and CPC on stress time and temperature. ANPC increases with both stress temperature and time, but CPC does not.

Fig. 8 shows that a positive charge built up without saturation as the stress time increases, although the interface states saturate. Fig. 9 shows that AHT also saturates. Fig. 12 shows that the generated ANPC is the only defect responsible for the non-saturation of threshold voltage instability against stress time.

V. CONCLUSION

In this paper, the impact of positive charging on the performance of pMOSFETs has been studied. Three components of threshold voltage instability are unambiguously identified, i.e., loop, loop-shift, and up-loop. When a pulse is applied to the gate, the TCs measured at the second edge of the pulse do not follow that at the first edge, leading to the formation of a loop. It dominates the V_{th} instability at relatively short time (< 1 s). For longer time, the whole loop is shifted in the negative direction, although the loop size changes little. Unlike the loop, the up-loop cannot readily be recharged after neutralization.

A framework has been proposed for the defect, and the relation between each type of defect and V_{th} instability is clarified. In addition to the generated interface states, three kinds of positive charge exist in Hf stacks, i.e., CPC, ANPC, and AHT. Each type of defect has its unique signatures and can

unambiguously be separated from the rest. CPC can repeatedly be charged and discharged by alternating the gate bias polarity. It is insensitive to measurement temperature and stress time, and is responsible for the loop. AHT is responsible for the up-loop, which is readily neutralized but not recharged at short stress time. As the stress time increases, it saturates. The loop-shift originates from both generated interface states and ANPC. ANPC is more difficult to neutralize than CPC and AHT, and is generated by the stress. It is the only defect that does not saturate with stress time and is responsible for the observed dependence of ΔV_{th} on the measurement temperature. This framework for positive charges is not process specific, although the magnitude of positive charges depends on the process condition.

REFERENCES

- [1] G. Groeseneken, L. Pantisano, L.-A. Ragnarsson, R. Degraeve, M. Houssa, T. Kauerauf, P. Roussel, S. De Gendt, and M. Heyns, "Achievements and challenges for the electrical performance of MOSFETs with high- k gate dielectrics," in *Proc. 11th Int. Symp. Phys. and Failure Anal. of IC*, 2004, pp. 147–155.
- [2] T. P. Ma, H. M. Bu, X. W. Wang, L. Y. Song, W. He, M. Wang, H.-H. Tseng, and P. J. Tobin, "Special reliability features for Hf-based high- κ gate dielectrics," *IEEE Trans. Device Mater. Rel.*, vol. 5, no. 1, pp. 36–44, Mar. 2005.
- [3] H. D. Xiong, D. Heh, M. Gurfinkel, Q. Li, Y. Shapira, C. Richter, G. Bersucker, R. Choi, and J. S. Suehle, "Characterization of electrically active defects in high- k gate dielectrics by using low frequency noise and charge pumping measurements," *Microelectron. Eng.*, vol. 84, no. 9/10, pp. 2230–2234, Sep/Oct. 2007.
- [4] J. H. Sim, S. C. Song, P. D. Kirsch, C. D. Young, R. Choi, D. L. Kwong, B. H. Lee, and G. Bersucker, "Effects of ALD HfO₂ thickness on charge trapping and mobility," *Microelectron. Eng.*, vol. 80, pp. 218–221, 2005.
- [5] C. Z. Zhao, J. F. Zhang, M. B. Zahid, B. Govoreanu, G. Groeseneken, and S. De Gendt, "Determination of capture cross sections for as-grown electron traps in HfO₂/HfSiO stacks," *J. Appl. Phys.*, vol. 100, no. 9, pp. 093716-1–093716-10, Nov. 2006.
- [6] A. Kerber, E. Cartier, L. Pantisano, M. Rosmeulen, R. Degraeve, T. Kauerauf, G. Groeseneken, H. E. Maes, and U. Schwalke, "Characterization of the V_T -instability in SiO₂/HfO₂ gate dielectrics," in *Proc. 41st Annu. Int. Reliab. Phys. Symp.*, 2003, pp. 41–45.
- [7] M. Houssa, S. De Gendt, J. L. Autran, G. Groeseneken, and M. M. Heyns, "Role of hydrogen on negative bias temperature instability in HfO₂-based hole channel field-effect transistors," *Appl. Phys. Lett.*, vol. 85, no. 11, pp. 2101–2103, Sep. 2004.
- [8] K. Onishi, R. Choi, C. S. Kang, H.-J. Cho, Y. H. Kim, R. E. Nieh, J. Han, S. A. Krishnan, M. S. Akbar, and J. C. Lee, "Bias-temperature instabilities of polysilicon gate HfO₂ MOSFETs," *IEEE Trans. Electron Devices*, vol. 50, no. 6, pp. 1517–1524, Jun. 2003.
- [9] H. R. Harris, R. Choi, B. H. Lee, C. D. Young, J. H. Sim, K. Mathews, P. Zeitzoff, P. Majhi, and G. Bersucker, "Comparison of NMOS and PMOS stress for determining the source of NBTI in TiN/HfSiO₂ devices," in *Proc. 43rd Int. Reliab. Phys. Symp.*, 2005, pp. 80–83.
- [10] H. R. Harris, R. Choi, J. H. Sim, C. D. Young, P. Majhi, B. H. Lee, and G. Bersucker, "Electrical observation of deep traps in high- κ /metal gate stack transistors," *IEEE Electron Device Lett.*, vol. 26, no. 11, pp. 839–841, Nov. 2005.
- [11] C. Z. Zhao, J. F. Zhang, M. B. Zahid, G. Groeseneken, R. Degraeve, and S. De Gendt, "Impact of gate materials on positive charge formation in HfO₂/SiO₂ stacks," *Appl. Phys. Lett.*, vol. 89, no. 2, p. 023507, Jul. 2006.
- [12] C. Z. Zhao, M. B. Zahid, J. F. Zhang, G. Groeseneken, R. Degraeve, and S. De Gendt, "Properties and dynamic behavior of electron traps in HfO₂/SiO₂ stacks," *Microelectron. Eng.*, vol. 80, pp. 366–369, Jun. 2005.
- [13] J. F. Zhang, C. Z. Zhao, M. B. Zahid, G. Groeseneken, R. Degraeve, and S. De Gendt, "An assessment of the location of as-grown electron traps in HfO₂/HiSiO stacks," *IEEE Electron Device Lett.*, vol. 27, no. 10, pp. 817–820, Oct. 2006.
- [14] A. Shanware, M. R. Visokay, J. J. Chambers, A. L. P. Rotondaro, J. McPherson, L. Colombo, G. A. Brown, C. H. Lee, Y. Kim, M. Gardner, and R. W. Murto, "Characterization and comparison of the

- charge trapping in HfSiON and HfO₂ gate dielectrics," in *IEDM Tech Dig.*, 2003, pp. 939–942.
- [15] D. R. Young, E. A. Irene, D. J. DiMaria, R. F. De Keersmaecker, and H. Z. Massoud, "Electron trapping in SiO₂ at 295 and 77 °K," *J. Appl. Phys.*, vol. 50, no. 10, pp. 6366–6372, Oct. 1979.
- [16] S. K. Lai and D. R. Young, "Effects of avalanche injection of electrons into silicon dioxide—Generation of fast and slow interface states," *J. Appl. Phys.*, vol. 52, no. 10, pp. 6231–6240, Oct. 1981.
- [17] D. M. Fleetwood, "Effects of hydrogen transport and reactions on microelectronics radiation response and reliability," *Microelectron. Reliab.*, vol. 42, no. 4/5, pp. 523–541, Apr./May 2002.
- [18] J. F. Zhang, C. Z. Zhao, A. H. Chen, G. Groeseneken, and R. Degraeve, "Hole-traps in silicon dioxides—Part I: Properties," *IEEE Trans. Electron Devices*, vol. 51, no. 8, pp. 1267–1273, Aug. 2004.
- [19] C. Z. Zhao, J. F. Zhang, G. Groeseneken, and R. Degraeve, "Hole-traps in silicon dioxides—Part II: Generation mechanism," *IEEE Trans. Electron Devices*, vol. 51, no. 8, pp. 1274–1280, Aug. 2004.
- [20] C. Z. Zhao and J. F. Zhang, "Effects of hydrogen on positive charges in gate oxides," *J. Appl. Phys.*, vol. 97, no. 7, pp. 073 703-1–073 703-8, Apr. 2005.
- [21] J. F. Zhang, H. K. Sii, G. Groeseneken, and R. Degraeve, "Hole trapping and trap generation in the gate silicon dioxide," *IEEE Trans. Electron Devices*, vol. 48, no. 6, pp. 1127–1135, Jun. 2001.
- [22] J. F. Zhang, H. K. Sii, G. Groeseneken, and R. Degraeve, "Degradation of oxides and oxynitrides under hot hole stress," *IEEE Trans. Electron Devices*, vol. 47, no. 2, pp. 378–386, Feb. 2000.
- [23] J. F. Zhang, S. Taylor, and W. Eccleston, "Electron trap generation in thermally grown SiO₂ under Fowler–Nordheim stress," *J. Appl. Phys.*, vol. 71, no. 2, pp. 725–734, Jan. 1992.
- [24] M. H. Chang and J. F. Zhang, "On positive charge formed under negative bias temperature stress," *J. Appl. Phys.*, vol. 101, no. 2, p. 024 516, Jan. 2007.
- [25] C. Tan, M. Xu, and Y. Wang, "Application of the difference subthreshold swing analysis to study generation interface trap in MOS structures due to Fowler–Nordheim aging," *IEEE Electron Device Lett.*, vol. 15, no. 7, pp. 257–259, Jul. 1994.
- [26] M. Denais, A. Bravaix, V. Huard, C. Parthasarathy, G. Ribes, F. Perrier, Y. Rey-Tauriac, and N. Revil, "On-the-fly characterization of NBTI in ultra-thin gate oxide PMOSFETs," in *IEDM Tech. Dig.*, 2004, pp. 109–112.
- [27] C. Shen, M.-F. Li, C. E. Foo, T. Yang, D. M. Huang, A. Yap, G. S. Samudra, and Y.-C. Yeo, "Characterization and physical origin of fast V_{th} transient in NBTI of pMOSFETs with SiON dielectric," in *IEDM Tech. Dig.*, 2006, pp. 333–336.
- [28] K. O. Jeppson and C. M. Svensson, "Negative bias stress of MOS devices at high electric fields and degradation of MNOS devices," *J. Appl. Phys.*, vol. 48, no. 5, pp. 2004–2014, May 1977.
- [29] J. F. Zhang, M. H. Chang, and G. Groeseneken, "Effects of measurement temperature on NBTI," *IEEE Electron Device Lett.*, vol. 28, no. 4, pp. 298–300, Apr. 2007.
- [30] B. Kaczer, T. Grasser, R. Fernandez, and G. Groeseneken, "Toward understanding the wide distribution of time scales in negative bias temperature instability," *ECS Trans. Silicon Nitride, Silicon Dioxide, Emerg. Dielectr.*, vol. 6, pp. 265–281, 2007.
- [31] S. S. Tan, T. P. Chen, J. M. Soon, K. P. Loh, C. H. Ang, and L. Chen, "Nitrogen-enhanced negative bias temperature instability: An insight by experiment and first-principle calculations," *Appl. Phys. Lett.*, vol. 82, no. 12, pp. 1881–1883, Mar. 2003.
- [32] M. H. Chang, Y. Wang, J. F. Zhang, C. Z. Zhao, W. D. Zhang, and M. Xu, "Contribution of as-grown hole traps to NBTI," *ECS Trans. Silicon Nitride, Silicon Dioxide, Emerg. Dielectr.*, vol. 6, pp. 245–262, 2007.
- [33] E. P. O'Reilly and J. Robertson, "Theory of defects in vitreous silicon dioxide," *Phys. Rev. B, Condens. Matter*, vol. 27, no. 6, pp. 3780–3795, Mar. 1983.
- [34] J. K. Rudra and W. B. Fowler, "Oxygen vacancy and the E₁' center in crystalline SiO₂," *Phys. Rev. B, Condens. Matter*, vol. 35, no. 15, pp. 8223–8230, May 1987.
- [35] M. H. Chang, J. F. Zhang, and W. D. Zhang, "Assessment of capture cross sections and effective density of electron traps generated in silicon dioxides," *IEEE Trans. Electron Devices*, vol. 53, no. 6, pp. 1347–1354, Jun. 2006.
- [36] K. Kushida-Abdelghafar, K. Watanabe, J. Ushio, and E. Murakami, "Effect of nitrogen at SiO₂/Si interface on reliability issues—Negative-bias-temperature instability and Fowler–Nordheim-stress degradation," *Appl. Phys. Lett.*, vol. 81, no. 23, pp. 4362–4364, Dec. 2002.
- [37] A. Stesmans and V. V. Afanas'ev, "Electrical activity of interfacial paramagnetic defects in thermal (100) Si/SiO₂," *Phys. Rev. B, Condens. Matter*, vol. 57, no. 16, pp. 10 030–10 034, Apr. 1998.
- [38] D. J. DiMaria, E. Cartier, and D. Arnold, "Impact ionization, trap creation, degradation, and breakdown in silicon dioxide films on silicon," *J. Appl. Phys.*, vol. 73, no. 12, pp. 3367–3384, Mar. 1993.



Ce Z. Zhao received the B.Eng. and M.Sc. degrees from Xidian University, Xi'an, China, in 1985 and 1992, respectively, and the Ph.D. degree in semiconductor physics and devices field from Xi'an Jiaotong University, Xi'an, in 1995.

He was a Professor with Xidian University. During his 13 years with Xidian University, he spent time doing research on semiconductor-integrated optics and waveguided devices. From July 1998 to January 2007, he was a Research Fellow with the Liverpool John Moores University, Liverpool, U.K.

Since January 2007, he has been a Research Associate with the University of Liverpool, Liverpool. His current research areas include deposit and characterization of high-*k* materials, and performance and degradation of MOS devices. He has authored or coauthored more than 50 publications in international scientific journals and international conference proceedings, and three books.

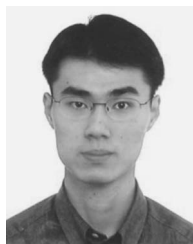


Jian F. Zhang received the B.Eng. degree in electrical engineering from the Xi'an Jiaotong University, Xi'an, China, in 1982 and the Ph.D. degree in electrical engineering from the University of Liverpool, Liverpool, U.K., in 1987.

From 1986 to 1992, he was a Senior Research Assistant with the University of Liverpool, where he worked on the dielectric recovery of plasma in accelerating gas flow, plasma processing of semiconductors, and the reliability of MOS devices. In 1992, he joined Liverpool John Moores University,

Liverpool, as a Senior Lecturer. He became a Reader in microelectronics in 1996 and a Professor since 2001. His current research interests include performance, degradation, and defect characterization of MOS devices and high-*k* layers.

Dr. Zhang was a member of the technical program committee for the IEEE Semiconductor Interface Specialists Conference and was invited to give talks at several international conferences.



Mo Huai Chang was born in Taipei, Taiwan, R.O.C., in 1978. He received the DUT degree in electrical and computer engineering from the Paris XI Cachan Institute of Technology, Paris, France, in 1999, and the B.Eng. degree in computer engineering and Ph.D. degree from Liverpool John Moores University, Liverpool, U.K., in 2000 and 2006, respectively.

He is currently a Post-Doctoral Research Assistant with Liverpool John Moores University. His present research interest includes defect generation in MOS dielectrics and the reliability of MOS devices.



A. R. Peaker received the B.Sc., M.Sc., Ph.D., and D.Sc. (in 1986) degrees from The University of Manchester, Manchester, U.K.

In 1967, he was with the semiconductor company Ferranti, where he was responsible for the development of the world's first commercial visible LEDs. He continued to work in the semiconductor industry in the U.K. and USA for ten years on III-V compounds and silicon materials. Then, he returned to The University of Manchester, where his work focused on defects in semiconductors. He became

a Professor of electronic materials in 1989 and Emeritus Professor in 2008. Of his 300 publications, about 200 are on defects in semiconductors and at semiconductor dielectric interfaces.

Dr. Peaker is a Fellow of the Institution of Engineering and Technology. He was awarded the 1993 National Physical Laboratory Prize for Measurement for his invention of Laplace deep-level transient spectroscopy and a Royal Academy of Engineering Foresight Award in 1997 to spend a year at the High Magnetic Field Lab, Grenoble, France, to develop novel techniques to study defects in electronic materials.



Stephen Hall (M'93) received the Ph.D. degree from the University of Liverpool, Liverpool, U.K., in 1987, for work on a new form of integrated injection logic in the GaAs/AlGaAs materials system.

He then took up a lecturing post and undertook work on silicon-on-insulator (SOI) materials characterization and device physics in SIMOX and oxidized porous Si systems. The work was in collaboration with U.K. universities and industrial collaborators. Other areas of activity concerned cobalt-disilicide Schottky diodes together with silicon-germanium Schottky diodes and device physics for both SOI HBT bipolar transistor and MOSFETs. He is currently the Head of the Department of Electrical Engineering and Electronics with the University of Liverpool. His current major activities concern novel design concepts for RF, vertical MOSFETs, micropower SOI circuits, high- k dielectrics for ultimate CMOS, and highly scalable device and circuit blocks for spiking neural-network application.

Dr. Hall currently serves on the technical program committee of the Insulating Films on Semiconductor Conference and is the Technical Program Chair of the European Solid-State Device Research Conference 2008.



Guido Groeseneken (F'05) received the M.Sc. degree in electrical and mechanical engineering and the Ph.D. degree in applied sciences from Katholieke Universiteit Leuven (KU Leuven), Leuven, Belgium, in 1980 and 1986, respectively.

In 1987, he was with the R&D Laboratory, Interuniversity Microelectronics Center (IMEC), Leuven, where, from October 2005 to April 2007, he was responsible for the IMEC Post-CMOS Nanotechnology Program and is currently engaged in research on reliability physics for deep submicrometer

CMOS technologies. Since 2001, he has also been a Professor with KU Leuven. He is the holder of ten patents. He is the author or coauthor of more than 300 publications in international scientific journals and conference proceedings, and six book chapters. His current research interests include the fields of nonvolatile semiconductor memory devices and technology, reliability physics of very-large-scale integration (VLSI) technology, hot carrier effects in MOSFETs, time-dependent dielectric breakdown of oxides, negative-bias-temperature instability effects, electrostatic discharge (ESD) protection and ESD testing, plasma-processing-induced damage, electrical characterization of semiconductors, and characterization and reliability of high- k dielectrics.

Dr. Groeseneken has been a member of the technical program committees of several international scientific conferences, including the IEEE International Electron Devices Meeting (IEDM), the European Solid-State Device Research Conference, the International Reliability Physics Symposium, the IEEE Semiconductor Interface Specialists Conference, and the Electrical Overstress/Electrostatic Discharge Symposium. From 2000 to 2002, he was the European Arrangements Chair of the IEDM. In 2005, he was the General Chair of the Insulating Films on Semiconductor Conference, Leuven.



Luigi Pantisano received the M.S. and Ph.D. degrees from the University of Padova, Padova, Italy, in 1996 and 2000, respectively, both in electrical engineering.

In 2000, he was with Bell Laboratories-Lucent Technologies, Murray Hill, NJ, where he worked on the impact of plasma-charging damage on RF CMOS devices. Since 2001, he has been with the Interuniversity Microelectronics Center, Leuven, Belgium, where he works on high- k gate dielectrics for CMOS technologies. He contributed more than 130 papers

in the field of plasma damage, RF measurements, reliability, and electrical characterization of novel high- k devices.

Dr. Pantisano is committee member of several conferences (IEEE Semiconductor Interface Specialists Conference, the International Reliability Physics Symposium, International Symposium on Advance Gate Stack Technology, International Conference on Microelectronic Test Structures).



Stefan De Gendt received the Bs.Sc., Ms.Sc. and Ph.D. degrees in chemistry from the University of Antwerp, Antwerp, Belgium.

During his Ph.D. work, he was with the Belgian Science Foundation (FWO). In 1996, he joined the Interuniversity Microelectronics Center (IMEC), Leuven, Belgium, as a Research Scientist to research and develop ultraclean processes for silicon cleaning and pretreatment. His main research topics dealt with metallic contamination control and development of ozonated chemistries. In 1999, he became involved

in the research program on alternative dielectric materials (high- k) for gate stack applications. Until 2006, he has been the Program Manager of IMEC's high- k and metalgate program, which involves partnership of several leading-edge IC and equipment manufacturers. In 2007, he became the Program Manager for IMEC's post-CMOS nano program, dealing with carbon nanotubes, semiconducting nanowires, and graphene. Since 2003, he has also been affiliated with the Chemistry Department, Katholieke Universiteit Leuven, Leuven. He has authored or coauthored over 150 publications.



Marc Heyns was born in Turnhout, Belgium, on November 16, 1956. He received the M.S. degree in applied sciences (electronics) and the Ph.D. degree from Katholieke Universiteit Leuven (KU Leuven), Leuven, Belgium, in 1979 and 1986, respectively. His Ph.D. thesis was entitled "Study of the charge trapping and degradation of thermally grown SiO₂ layers."

From 1979 to 1985, he held a fellowship with the National Fund for Scientific Research (NFWO) in the Laboratory for Physics and Electronics of Semiconductors, KU Leuven. In January 1986, he joined the Interuniversity Microelectronics Center (IMEC), Leuven, where he became the Department Director and Program Director, and is responsible for a research group working on ultraclean processing technology, advanced high- k gate stacks, metal gates, epitaxial deposition of materials, environmentally benign processing, and novel high-mobility substrate materials. He became an IMEC Fellow in 2001 and a Professor with KU Leuven in 2005. He has authored or coauthored more than 180 publications in scientific peer-reviewed journals, more than 600 contributions at scientific conference proceedings, including more than 80 invited presentations, and has edited or contributed to various books. His current research topics include novel high- k dielectric materials, advanced cleaning and surface preparation technology, epitaxy, novel devices made on high-mobility substrates such Ge and III/V compounds, nanowires, and carbon nanotubes.